ONLINE TRAFFIC LIGHT CONTROL THROUGH GRADIENT ESTIMATION USING STOCHASTIC FLUID MODELS

Christos G. Panayiotou * **William C. Howell** **,[1]
Michael Fu ***,[2]

* *Department of Electrical and Computer Engineering, University of Cyprus, Nicosia, Cyprus*
christosp@ucy.ac.cy
** *Department of Mathematics, Applied Mathematics Scientific Computation Program, University of Maryland, College Park, MD 20742, USA.* wch@math.umd.edu
*** *Smith School of Business and Institute for Systems Research, University of Maryland, College Park, MD 20742, USA.* mfu@isr.umd.edu

Abstract: In this paper, we consider the problem of dynamically regulating the timing of traffic light controllers in busy cities. We use a Stochastic Fluid Model (SFM) to model the dynamics of the queues formed at an intersection. Based on this model, we derive gradients of the queue lengths with respect to the green/red light lengths within a signal cycle. We derive both a simple and a periodic model and report preliminary numerical results comparing the performance of the estimates with finite-difference and smoothed perturbation analysis estimates. Then all estimators are used to optimize the traffic system via Stochastic Approximation.

Keywords: Traffic control, perturbation analysis, stochastic approximation, stochastic systems.

1. INTRODUCTION

In this paper we consider the problem of easing traffic congestion by dynamically adjusting the timing of the traffic light that regulates the vehicle flow at a single intersection. This is a problem that over the years has attracted the attention of several researchers and many approaches have been proposed. In (Moskowitz *et al.*, 1997) the authors propose a model for estimating the traffic conditions based on measured information. In (Hoyer and Jumar, 1994) the authors develop a fuzzy controller. In (De Schutter, 1999) the author formulates an Extended Linear Complementary Problem (ELCP) and (Zhao and Chen, 2003) uses a formulation based on hybrid systems. Finally, in (L. Head, 1996) the authors use a Perturbation Analysis framework ((Ho and Cao, 1991)) and in (Fu and Howell, 2003) Smoothed Perturbation Analysis (SPA (Gong and Ho, 1987)). In this paper, we also use Infinitesimal Perturbation and Analysis (IPA) but the model we use to derive the

[1] Supported in part by the National Science Foundation under Grant DMI-9988867 and by the United Negro College Fund Special Programs under the NASA Harriet G. Jenkins Predoctoral Fellowship Program.
[2] Supported in part by the National Science Foundation under Grant DMI-9988867 and by the Air Force Office of Scientific Research under Grant F496200110161.

IPA estimates is a Stochastic Fluid Model (SFM). Subsequently, when we evaluate the estimators, we use observations from the actual discrete-event model. Though stochastic fluid models might not be very accurate for *performance evaluation*, they have proven to be very robust with respect to *optimization* because they seem to capture the salient features of the problem. Several authors have reported that use of SFM efficiently lead to optimal or near-optimal solutions (see (Cassandras *et al.*, 2002; Meyn, 2000; Sun *et al.*, 2003) and references therein). Using the SFM modeling framework, a new approach for resource management is being developed which is based on IPA (Cassandras *et al.*, 2002). In this approach, we derive estimators of the gradient of the performance measure of interest with respect to the control parameters of interest based on SFMs. Then we evaluate them based on observations on the actual Discrete-Event System (DES) and use resulting estimates with stochastic approximation algorithms to determine the optimal parameter setting. This approach has some very important advantages.

- The gradient estimation is done *on-line* thus the approach can be implemented on the traffic light controller and as operating conditions change, it will aim at *continuously* seeking to optimize a generally time-varying performance metric (This holds for both SPA and SFM-Based estimators).
- Unlike the SPA estimators, SFM-based estimators do *not* require any knowledge of the system's underlying stochastic processes.
- SFM-Based IPA estimators are generally simpler to implement than SPA
- SPA estimators are generally more accurate than the SFM-Based IPA estimators but simulation results indicated that in optimization problems they perform equally well.

For this paper, the performance measure of interest is the average number of cars waiting at the traffic light signal for a particular intersection, so for $q = 1, 2$ we define $L_q(t;\theta)$ to be the number of cars waiting on street q at time t and $\bar{L}_q(t;\theta)$ is the average $L_q(t;\theta)$ up to time t, i.e.,

$$\bar{L}_q(t;\theta) = \frac{1}{t}\int_0^t L_q(x;\theta)dx.$$

With θ denoting a parameter of interest, we wish to derive estimators for

$$\frac{dE[\bar{L}_q(t;\theta)]}{d\theta}, \quad q = 1, 2.$$

For this paper, we assume that the length of the green light period (T_1) and red light period (T_2) are constant, and thus take θ as either T_1 or T_2. A complete cycle (T) constitutes the completion of a green and red light period. T is held fixed, thus a positive perturbation in T_1 will result in a negative perturbation in T_2 and vice versa (note that extensions are possible to make T also a control parameter).

Furthermore, we let $x_q(t;\theta)$, $q = \{1, 2\}$ denote the *fluid* buffer content of each queue in the interval $t \in [0, S]$ and we define the sample functions

$$Q_q(t;\theta) = \frac{1}{t}\int_0^t x_q(\tau;\theta)d\tau. \tag{1}$$

Then we derive sample derivatives of $Q_q(t;\theta)$ with respect to θ using two different SFMs. Recall that $\bar{L}_q(t;\theta)$ and $Q_q(t;\theta)$ correspond to the average queue levels up to t at street q of the stochastic discrete-event and stochastic fluid models respectively. We take $Q_q(t;\theta)$ as an approximation of $\bar{L}_q(t;\theta)$. Using IPA, $\frac{dQ_q(t;\theta)}{d\theta}$ is derived. These IPA estimators of $\frac{dQ_q(t;\theta)}{d\theta}$ are used to approximate $\frac{dE[\bar{L}_q(t;\theta)]}{d\theta}$.

2. SIMPLE MODEL

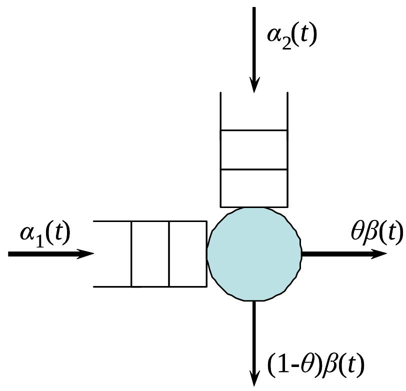

Fig. 1. Simple Model

Fig. 1 shows the equivalent queuing model where the processing capacity of the server ($\beta(t)$) is divided between the two queues with proportions θ and $(1-\theta)$ respectively. Fig. 2 shows a typical sample path of the system. Clearly, this model is not representative of the traffic flow at an intersection. Using this modeling framework we don't consider the specific scheduling policy used by the traffic light server (this will be done in the next section). Here we assume a fluid model where fluid is processed from both queues simultaneously at proportions θ and $(1-\theta)$. However, we decided to evaluate it just to see whether it also captures the salient features of the problem and can also be used in optimization (as we will see in Section 4 this is not the case).

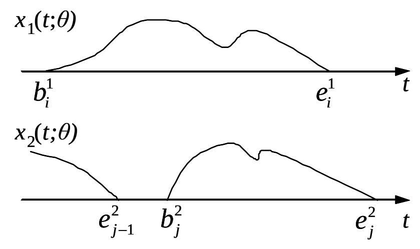

Fig. 2. Typical sample path

2.1 Sample Path Partition

For this model we partition the sample path into empty and non-empty periods. Empty periods are maximal intervals where $x_q(t;\theta) = 0$ while non-empty intervals indicate the intervals such that $x_q(t;\theta) > 0$, $q = \{1, 2\}$. Let $\bar{E}_i^q = (b_i^q, e_i^q)$ indicate the ith non-empty period, where b_i^q indicates the beginning and e_i^q the end of the ith non-empty period at queue $q = \{1, 2\}$. Using this notation, the sample functions (1) can be written as

$$Q_q(S;\theta) = \frac{1}{S}\sum_{j=1}^{N_q} q_j(S;\theta) = \frac{1}{S}\sum_{j=1}^{N_q}\int_{b_j^q}^{e_j^q} x_q(t;\theta)dt \quad (2)$$

where N_q denotes the random number of non-empty periods in the interval $[0, S]$. Differentiating with respect to θ we get

$$\frac{dQ_q(\theta)}{d\theta} = \frac{1}{S}\sum_{j=1}^{N_q}\frac{dq_j(\theta)}{d\theta} = \frac{1}{S}\sum_{j=1}^{N_q}\int_{b_j^q}^{e_j^q}\frac{dx_q(t;\theta)}{d\theta}dt \quad (3)$$

since $x_q(b_j^q, \theta) = x_q(e_j^q, \theta) = 0$ for $q = \{1, 2\}$ and $j = 1, 2, \cdots$. In any interval $\bar{E}_j^1 = (b_j^1, e_j^1)$, the buffer content $x_1(t;\theta)$ is given by

$$x_1(t;\theta) = \int_{b_j^1}^{t}(\alpha_1(\tau) - \theta\beta(\tau))d\tau \quad (4)$$

Lemma 2.1. The derivative of $x_1(t;\theta)$ with respect to θ is given by

$$\frac{dx_1(t;\theta)}{d\theta} = -\int_{b_j^1}^{t}\beta(\tau)d\tau \quad (5)$$

The proof of all lemmas and theorems are omitted due to space limitations. For the convenience of the reviewers however, they are placed in an appendix.

Similarly, for $q = 2$ we have

$$x_2(t;\theta) = \int_{b_j^2}^{t}(\alpha_2(\tau) - (1-\theta)\beta(\tau))d\tau \quad (6)$$

and by differentiation (similarly to Lemma 2.1) we obtain the following result

Lemma 2.2. The derivative of $x_2(t;\theta)$ with respect to θ is given by

$$\frac{dx_2(t;\theta)}{d\theta} = +\int_{b_j^2}^{t}\beta(\tau)d\tau \quad (7)$$

Next, substituting (5) and (7) back in (3) we get the following result

Theorem 2.1. The sample derivatives for the workload are given by

$$\frac{dQ_1(\theta)}{d\theta} = -\frac{1}{S}\sum_{j=1}^{N_1}\int_{b_j^1}^{e_j^1}\int_{b_j^1}^{t}\beta(\tau)d\tau dt \quad (8)$$

$$\frac{dQ_2(\theta)}{d\theta} = \frac{1}{S}\sum_{j=1}^{N_2}\int_{b_j^2}^{e_j^2}\int_{b_j^2}^{t}\beta(\tau)d\tau dt \quad (9)$$

Example: Next, let us consider a simple example where $\beta(t) = \beta$ (constant). In this case, it is straight forward to show that

$$\frac{dQ_1(\theta)}{d\theta} = -\frac{\beta}{2S}\sum_{j=1}^{N_1}\left(e_j^1 - b_j^1\right)^2. \quad (10)$$

Similarly,

$$\frac{dQ_2(\theta)}{d\theta} = \frac{\beta}{2S}\sum_{j=1}^{N_2}\left(e_j^2 - b_j^2\right)^2. \quad (11)$$

Note that these estimators ((10) and (11)) are extremely simple to implement. We just accumulate the squares of the duration of each non-empty period.

3. PERIODIC MODEL

Fig. 3 shows a perhaps more relevant fluid model where the *entire* server capacity is allocated to the first queue for a period $0 < \theta < T$ and to the second queue for a period $0 < T - \theta < T$. In this model, T indicates the period of one cycle from ‘green’ to ‘red’. Fig. 4 shows a typical sample path due to this model.

3.1 Sample Path Partition

In this modeling approach the sample path is divided into intervals of length T and the dynamics of the two queues are described as follows

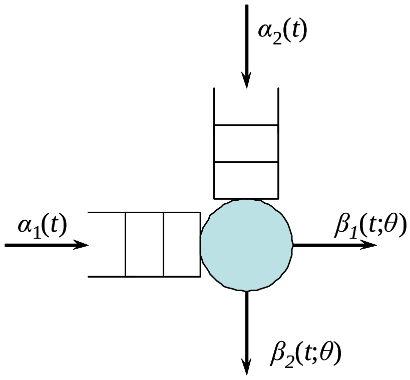

Fig. 3. Periodic Model

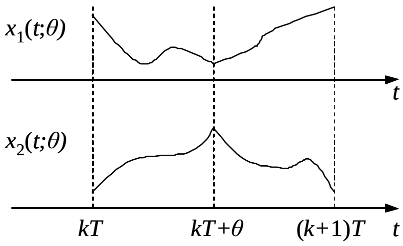

Fig. 4. Typical sample path for the periodic model

$$\frac{dx_1(t;\theta)}{dt} = \begin{cases} \alpha_1(t) - \beta_1(t;\theta), \\ \quad \text{if } kT \le t < kT + \theta \\ \alpha_1(t), \\ \quad \text{if } kT + \theta \le t < (k+1)T \end{cases} \tag{12}$$

$$\frac{dx_2(t;\theta)}{dt} = \begin{cases} \alpha_2(t), \\ \quad \text{if } kT \le t < kT + \theta \\ \alpha_2(t) - \beta_2(t;\theta), \\ \quad \text{if } kT + \theta \le t < (k+1)T \end{cases} \tag{13}$$

$k = 1, 2, \cdots$. In addition, the service rates are defined as

$$\beta_1(t;\theta) = \begin{cases} \rho_1(t), & \text{if } kT \le t < kT + \theta \\ & \text{and } x_1(t;\theta) > 0 \\ \alpha_1(t), & \text{if } kT \le t < kT + \theta \\ & \text{and } x_1(t;\theta) = 0 \\ 0, & \text{otherwise} \end{cases} \tag{14}$$

$$\beta_2(t;\theta) = \begin{cases} \rho_2(t), \\ \quad \text{if } kT + \theta \le t < (k+1)T \\ \quad \text{and } x_2(t;\theta) > 0 \\ \alpha_2(t), \\ \quad \text{if } kT + \theta \le t < (k+1)T \\ \quad \text{and } x_2(t;\theta) = 0 \\ 0, \quad \text{otherwise} \end{cases} \tag{15}$$

where $\rho_1(t)$ and $\rho_2(t)$ are the maximum possible outflows from queues 1 and 2 respectively. The sample functions of (1) can be written as

$$Q_q(\theta) = \frac{1}{S}\sum_{k=1}^{K} \phi_k^q(\theta) = \frac{1}{S}\sum_{k=1}^{K} \int_{kT}^{(k+1)T} x_q(t;\theta)dt \tag{16}$$

where K is the number of periods included in the interval $[0, S]$ and the index $q \in \{1, 2\}$. Differentiating with respect to θ we get

$$\frac{dQ_q(\theta)}{d\theta} = \frac{1}{S}\sum_{k=1}^{K} \frac{d\phi_k^q(\theta)}{d\theta} = \frac{1}{S}\sum_{k=1}^{K} \int_{kT}^{(k+1)T} \frac{dx_q(t;\theta)}{d\theta}dt. \tag{17}$$

For simplicity, let us first try to evaluate a single term from the summation for $q = 1$, i.e.,

$$\frac{d\phi_k^1(\theta)}{d\theta} = \int_{kT}^{(k+1)T} \frac{dx_1(t;\theta)}{d\theta}dt.$$

Given the queue dynamics of (12), we determine the queue content depending on the interval that t falls in:

Case A: $(kT \le t < kT + \theta)$ This interval is further divided into two more subcases depending on the observation of an empty period. Here we also make an assumption that during a period of 'green' light, if the queue becomes empty, then it will not become non-empty until the next 'red' light.

A1: The queue does *not* become empty during this period

$$x_1(t;\theta) = x_1(kT;\theta) + \int_{kT}^{t} (\alpha_1(t) - \rho_1(t))\, dt \tag{18}$$

A2: The queue becomes empty during the period

$$x_1(t;\theta) = \begin{cases} x_1(kT;\theta) + \int_{kT}^{t} (\alpha_1(t) - \rho_1(t))\, dt, \\ \qquad \text{if } kT \le t < e_j^1 \\ 0, \quad \text{if } e_j^1 \le t < (k+1)T \end{cases} \tag{19}$$

Case B: $(kT + \theta \le t < (k+1)T)$

$$x_1(t;\theta) = x_1(kT + \theta;\theta) + \int_{kT+\theta}^{t} \alpha_1(t)dt \tag{20}$$

Summarizing, we get

$$x_1(t;\theta) = \begin{cases} x_1(kT;\theta) + \int_{kT}^{t} \alpha_1(t) - \rho_1(t)dt, \\ \qquad \text{if } kT \le t < e_{j_k}^1 \\ 0, \quad \text{if } e_{j_k}^1 \le t < kT + \theta \\ x_1(kT+\theta;\theta) + \int_{kT+\theta}^{t} \alpha_1(t)dt, \\ \qquad \text{if } kT + \theta \le t < (k+1)T \end{cases} \tag{21}$$

where, $e_{j_k}^1$ indicates the time when the buffer empties during the kth period. If no such event occurs, then we set $e_{j_k}^1 = (kT + \theta)$, thus the second case does not occur. Next, differentiating (21) we get

$$\frac{dx_1(t;\theta)}{d\theta} = \begin{cases} \dfrac{dx_1(kT;\theta)}{d\theta}, & \text{if } kT \le t < e^1_{j_k} \\ 0, \quad \text{if } e^1_{j_k} \le t < kT+\theta \\ \dfrac{dx_1(kT+\theta;\theta)}{d\theta} - \alpha_1(kT+\theta), \\ \qquad \text{if } kT+\theta \le t < (k+1)T \end{cases} \tag{22}$$

In other words, the derivative $\frac{dx_1(t;\theta)}{d\theta}$ is a piecewise constant function. Even though it may look complicated, this function is very easy to implement iteratively using a single accumulator! As a result, the derivative $\frac{dQ_1(\theta)}{d\theta}$ is also very easy to evaluate; it is just the derivative times the corresponding intervals.

$$\begin{aligned} \frac{dQ_1(\theta)}{d\theta} &= \frac{1}{S}\sum_{k=1}^{K}(e^1_{j_k} - kT)\frac{dx_1(kT;\theta)}{d\theta} \\ &+(T-\theta) \\ &\times \left(\frac{dx_1(kT+\theta;\theta)}{d\theta} - \alpha_1(kT+\theta)\right) \end{aligned} \tag{23}$$

where as mentioned earlier, $e^1_{j_k}$ is the time that buffer 1 empties during the interval $[kT, kT+\theta)$ and if no such event occurs, then $e^1_{j_k} = kT+\theta$. $\frac{dQ_2(\theta)}{d\theta}$ can be derived in a similar fashion.

4. RESULTS

In this section, we use simulation to acquire numerical results for the SFM estimators derived in this paper. These estimators along with the SPA estimators are then compared to finite difference estimates. All Simulation results are based on the following scenarios. In all cases, the interarrival and service time distributions were exponentially distributed, the number of cycles (N) was 10,000, and the number of replications was also 10,000. The first case (C1) had parameter values:

- respective mean interarrival and service times of 4.5 and 2.0;
- green length is 30.0 and total cycle length is 60.0.

The second case (C2) had parameter values:

- respective mean interarrival and service times of 5.0 and 1.5;
- green length is 35.0 and total cycle length is 110.0.

The third case (C3) had parameter values:

- respective mean interarrival and service times of 3.5 and 0.5;
- green length is 20.0 and total cycle length is 40.0.

The fourth case (C4) had parameter values:

- respective mean interarrival and service times of 10.5 and 5.0;
- green length is 20.0 and total cycle length is 40.0.

Estimators were simulated for all 4 cases; however, the optimization was carried out of C1, C2 and C3.

4.1 Stochastic Fluid Model Estimators

The simple model estimators (10) and (11) were implemented on the underlying stochastic DES model where for β we used the mean service rate of the server. As indicated in the simulation results (labelled SFM1), these estimators did not work well partly because the service rate of the buffer was not fixed and deterministic (as assumed by this SFM model) and partly because this model sis not capture the fact that at any queue, during the "red" light period, the service rate is 0.

The Periodic model was also implemented on the underlying DES stochastic model where for the instantaneous arrival rates $\alpha_q(t)$ in (23) we simply used the average arrival rate. The results for this model are labelled SFM2. In addition, we noticed that the assumption that the models stays empty once is empties causes the estimator to be low because in general the queue can become non-empty again during the same green-light cycle. We made a slight modification to the estimator to allow for arrivals to the queue during a green light phase while the system is empty. Instead of resetting $\frac{dx(kT;\theta)}{d\theta}$ whenever the system empties, we only reset when the system is empty at the epoch of the light change. This make intuitive sense because the perturbation only can propagate through the cycle if the system is nonempty. The results of the modified estimators are labelled SFM2mod.

4.2 Smoothed Perturbation Analysis (SPA)

Following the framework of (Fu and Hu, 1997), the general SPA estimator consists of an IPA term and a conditional term, the latter due to possible critical event order change. The SPA estimator is

$$\left(\frac{dE[\bar{L}]}{d\theta}\right)_{SPA} = \frac{d\bar{L}}{d\theta} + \lim_{\Delta\theta\to 0}\frac{P(\beta(\Delta\theta))}{\Delta\theta}\delta\bar{L}(\beta), \tag{24}$$

where $\beta(\Delta\theta)$ denotes a critical event change due to a perturbation of $\Delta\theta$, and $\delta\bar{L}(\beta)$ denotes the corresponding expected change in the performance measure $\bar{L}$.

Using this general form we derived four estimators, left and right-hand estimators for both queues. Here we state two of the SPA estimators. The details of the derivation are provided in (Howell and Fu, 2003). The right-hand estimator for queue 1 is

$$\left(\frac{dE[\bar{L}_1]}{d\theta}\right)_{SPA,r} = \frac{1}{NT}\sum_{i=1}^{N}\frac{f_1(\alpha_i)}{1-F_1(\alpha_i)}\left[-R_{q_i}^{(1)}\right]$$

where α_i is the time until light change (from green to red) from last entry to service during ith cycle, $R_n^{(i)}$ is the expected time to empty queue i, given n cars in the queue, q_i is the number in queue at the epoch of the ith light change from green to red, f_i is the service time density and F_i is the service time distribution.

The left-hand estimator for queue 2 is

$$\left(\frac{dE[\bar{L}_2]}{d\theta}\right)_{SPA,l} = \frac{1}{NT}\sum_{i=1}^{N}H_i + \frac{1}{NT}\sum_{i=1}^{N}\frac{f_2(\alpha_i)}{1-F_2(\alpha_i)}\left[R_{q_i}^{(2)}\right],$$

where H_i is the number of "critical" departures in cycle i. In the results, we denote SPA(RH) and SPA(LH) as the right hand and left hand SPA estimators respectively. Finally, FD denotes the finite difference results.

4.3 Stochastic Approximation

Stochastic Approximation (SA) is a gradient-based stochastic optimization algorithm, where the "best guess" of the optimal parameter is updated iteratively based on the estimate of the gradient of the performance measure with respect to the parameter (ref.(Fu and Hu, 1997)). The general form of SA is as follows,

$$t_{n+1}^* = \prod_{(0,t_p)}(t_n^* - a_n \nabla J_n), \tag{25}$$

where t_n^* is the parameter value at the beginning of iteration n, a_n is a positive sequence of step sizes, ∇J_n is the estimate of $\nabla J_n(t_n^*)$, the gradient of J_n at parameter value t_n^* and, $\prod_\Omega$ is the projection onto Ω. $\prod_\Omega$ keeps the parameter within the valid range of values. In this implementation of the SA algorithm, $\prod_\Omega$ returns the parameter back to he stable region if the update has caused some parameter to move outside of the stable region. From queuing theory, for queue stability we need $\lambda_1 \times T < \mu_1 \times T_1$ and $\lambda_2 \times T < \mu_2 \times (T - T_1)$. Thus, we have as our stable region the following

$$\frac{\lambda_1}{\mu_1} \times T < T_1 < T \times (1 - \frac{\lambda_2}{\mu_2}). \tag{26}$$

Table 1. Results for Case 1: $dE[\bar{L}_1]/d\theta$

estimator	mean	std err
SPA (RH)	-2.465	0.001
SPA (LH)	-2.465	0.001
FD (.05)	-2.475	0.024
SFM1	-147.82	0.154
SFM2	-1.713	0.002
SFM2mod	-2.188	0.006

Table 2. Results for Case 2: $dE[\bar{L}_1]/d\theta$

estimator	mean	std err
SPA (RH)	-8.3904	0.0061
SPA (LH)	-8.3835	0.0066
FD (.05)	-8.2115	0.0356
SFM1	-915.4631	1.4496
SFM2	-0.1683	0.0000
SFM2mod	-0.2412	0.0000

Table 3. Results for Case 3: $dE[\bar{L}_1]/d\theta$

estimator	mean	std err
SPA (RH)	-0.1717	0.0000
SPA (LH)	-0.1716	0.0001
FD (.05)	-0.1716	0.0003
SFM1	-11.1422	0.0004
SFM2	-0.1674	0.0000
SFM2mod	-0.1960	0.0000

Table 4. Results for Case 4: $dE[\bar{L}_1]/d\theta$

estimator	mean	std err
SPA (RH)	-20.8959	0.0424
SPA (LH)	-20.8848	0.0417
FD (.05)	-20.2334	0.1146
SFM1	-775.8161	4.0491
SFM2	-19.0584	0.0979
SFM2mod	-19.7437	0.0989

4.3.1. Gradient Estimation The results are shown in Tables 1, 2, 3 and 4. A comparison of the results shows that the simple model estimator (SFM1) is large in magnitude compared to the other estimates. We take the FD estimate as the true value in Table 5 to compare the percent error of each estimator. The left and right hand estimates are extremely accurate. Both the Periodic (SFM2) and the modified Periodic (SFM2mod) models provide fair estimates of the gradient. The standard error for the four aforementioned estimators is always less than that for the FD estimates. Even though the estimates do not match the FD estimates exactly, they still look promising for the system optimization.

4.3.2. Optimization We noticed that the SFM gradient estimated were not very accurate; however, from Fig. 5 we can see that the estimates have a very important quality. These gradient estimates are 0 at the minimum of the function. This is a good sign that the SFM estimates can be used for optimization via a gradient descent algorithm such as SA. All six gradient estimation techniques cross 0 at the minimum of $\bar{L}$. Fig. 5 shows this

Table 5. Percent error of estimators with FD as true value

estimator	case 1 % error	case 2 % error
SPA (RH)	-0.72%	2.18%
SPA (LH)	-0.70%	2.10%
FD (.05)	0.00%	0.00%
SFM1	6170.05%	11048.61%
SFM2	-30.86%	-97.95%
SFM2mod	-11.87%	-97.06%
estimator	case 3 % error	case 4 % error
SPA (RH)	0.09%	3.27%
SPA (LH)	0.03%	3.22%
FD (.05)	0.00%	0.00%
SFM1	6393.84%	3734.33%
SFM2	-2.45%	-5.81%
SFM2mod	14.21%	-2.42%
estimator	avg abs error	
SPA (RH)	1.57%	
SPA (LH)	1.51%	
FD (.05)	0.00%	
SFM1	6836.71%	
SFM2	34.27%	
SFM2mod	31.39%	

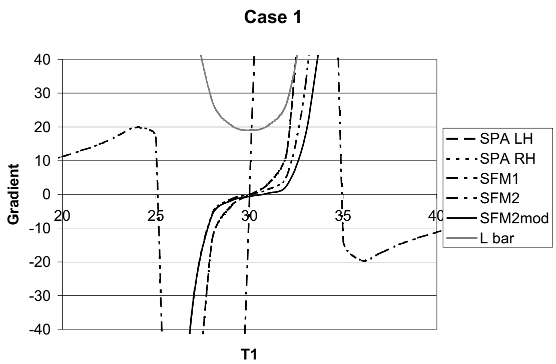

Fig. 5. Gradient Estimation Methods vs $\bar{L}$

for C1, the same property of the estimators was exhibited for C2 and C3 as well.

Because SA is an iterative algorithm, not only are we concerned with reaching the optimum, but we would like to stay near the optimum for subsequent updates. Therefore, we ran simulations and counted the number of times the average number in system was with p% (for p = 10,5,1) of the minimum average number in system based on the current T_1 from the SA algorithm. We label the three ranges as

- 10%-range : within 10% of the optimal $\bar{L}$
- 5%-range : within 5% of the optimal $\bar{L}$
- 1%-range : within 1% of the optimal $\bar{L}$.

All six gradient estimation techniques were implemented in the SA algorithm for cases C1, C2 and C3. Tables 6,7 and 8 show the number of times

Table 6. Number of times in optimum range for C1

estimator	10%	5%	1%
SPA (RH)	77.0	46.4	10.9
SPA (LH)	77.8	45.6	10.9
FD (.05)	76.5	45.0	10.1
SFM1	48.9	30.2	5.7
SFM2	79.3	47.9	10.9
SFM2mod	73.6	45.0	10.0

Table 7. Number of times in optimum range for C2

estimator	10%	5%	1%
SPA (RH)	92.9	89.9	60.1
SPA (LH)	92.7	90.2	61.0
FD (.05)	94.0	91.8	57.0
SFM1	3.0	2.6	1.2
SFM2	95.9	94.3	66.3
SFM2mod	95.1	91.3	10.9

Table 8. Number of times in optimum range C3

estimator	10%	5%	1%
SPA (RH)	43.0	21.8	4.6
SPA (LH)	43.1	22.4	4.2
FD (.05)	41.2	19.9	3.9
SFM1	43.0	21.7	4.7
SFM2	48.3	26.4	4.7
SFM2mod	42.9	21.7	4.6

each estimation fell within the aforementioned optimum ranges.

5. CONCLUSIONS AND FUTURE WORK

SFMs are promising for the purpose of *control and optimization* rather than *performance analysis*. In this paper we have shown that even if the exact gradient cannot be obtained by such "lower-resolution" models, one can still obtain near-optimal points that exhibit robustness with respect to certain aspects of the model they are based on. For this reason we believe that these SFM IPA gradient estimates can used to optimize the traffic model. We are currently incorporating the estimates from this paper into stochastic approximation optimization algorithms. The results thus far are promising. Next we will consider the application of the SFM estimator method to a network of intersections controlled by traffic lights.

REFERENCES

Cassandras, C. G., Y. Wardi, B. Melamed, G. Sun and C. G. Panayiotou (2002). Perturbation analysis for on-line control and optimization of stochastic fluid models. *IEEE Transactions on Automatic Control* **47**(8), 1234–1248.

De Schutter, Bart (1999). Optimal traffic light control for a single intersection. In: *Proceedings of the IEEE American Control Conference*. Vol. 3. pp. 2195 – 2199.

Fu, M.C. and J.Q. Hu (1997). *Conditional Monte Carlo: Gradient Estimation and Optimization Applications*. Kluwer Academic Publishers. Boston, Massachusetts.

Fu, M.C. and W.C. Howell (2003). Application of perturbation analysis to traffic light signal timing. In: *Proceedings of IEEE Conference on Decision and Control*.

Gong, W.B. and Y.C. Ho (1987). Smoothed perturbation analysis of discrete-event dynamic systems. *IEEE Transactions on Automatic Control* **32**, 858–867.

Ho, Y.C. and X.R. Cao (1991). *Perturbation Analysis of Discrete Event Dynamic Systems*. Kluwer. Boston, MA.

Howell, W.C. and M.C. Fu (2003). Optimizing traffic light signal timing using perturbation analysis. Working paper.

Hoyer, Robert and Ulrick Jumar (1994). Fuzzy control of traffic lights. In: *Proceedings of the IEEE World Congress on Computational Intelligence*. Vol. 3. pp. 1526 – 1531.

L. Head, F.W. Ciarallo, D. Lucas V. Kaduwela (1996). A perturbation analysis approach to traffic signal optimization. In: *INFORMS National Meeting*.

Meyn, S. (2000). Sequencing and routing in multiclass networks. Part I: Feedback regulation. In: *Proceedings of the IEEE International Symposium on Information Theory*. pp. 4440–4445. To appear in SIAM J. Control and Optimization.

Moskowitz, S., E. Fernández-Gaucherand and M. Whalen (1997). Passage-detector-based traffic queue estimation in intelligent transportation systems: A computational study of competing algorithms. *Applied Mathematics and Computation* **86**, 93–113.

Sun, G., C.G. Cassandras, Y. Wardi, C.G. Panayiotou and G Riley (2003). Perturbation analysis and optimization of stochastic flow networks. To appear.

Zhao, X. and Y. Chen (2003). Traffic light control method for a single intersection based on hybrid systems. In: *Proceedings of the IEEE Intelligent Transportation Systems*. pp. 1105 – 1109.

Proof of Lemma 2.1

The result of the differentiation is

$$\frac{dx_1(t;\theta)}{d\theta} = -\left(\alpha_1(b_j^1) - \theta\beta(b_j^1)\right)\frac{db_j^1}{d\theta} - \int\limits_{b_j^1}^{t} \beta(\tau)d\tau$$

since $\frac{dt}{d\theta} = 0$. However, we point out that the first term vanishes. This is shown as follows. Any point b_j^1 is such that $\alpha_1(b_j^{1-}) - \theta\beta(b_j^{1-}) \leq 0$ and $\alpha_1(b_j^{1+}) - \theta\beta(b_j^{1+}) \geq 0$. The sign switch can occur in one of two ways, either continuously or discontinuously. If it occurs in a continuous fashion then the above relations imply that $\alpha_1(b_j^1) - \theta\beta(b_j^1) = 0$. On the other hand, if it occurs in a discontinuous fashion, implies that the sign switch is due to a discontinuity either in $\alpha(b_j^1)$ or $\beta(b_j^1)$ which are independent of θ. Thus $\frac{db_j^1}{d\theta} = 0$ so the term again vanishes. ∎